RSC Advances

Homogeneous precipitation synthesis and electrochemical performance of LiFePO4/CNTs/C composite as advanced cathode materials for lithium ion batteries

Journal:	*RSC Advances*
Manuscript ID	RA-ART-10-2015-021384.R1
Article Type:	Paper
Date Submitted by the Author:	24-Nov-2015
Complete List of Authors:	Zhu, Peipei; University of Nanchang, Chemistry Yang, Zhen-Yu; University of Nanchang, Chemistry Zeng, Peng; University of Nanchang, Chemistry Zhong, Jing; Harbin Institute of Technology Yu, Ji; University of Nanchang, Chemistry Cai, Jianxin; University of Nanchang, Chemistry
Subject area & keyword:	Composites < Materials

Homogeneous precipitation synthesis and electrochemical performance of $LiFePO_4$/CNTs/C composite as advanced cathode materials for lithium ion batteries

Zhu Peipei[a], Zhenyu Yang[a,1], Peng Zeng[a], Jing Zhong[b], Ji Yu[a], and Jianxin Cai[a,1]

[a]*Department of Chemistry, Nanchang University, No. 999, Xuefu Road, New District of Honggutan, Nanchang, Jiangxi, 330031, P. R. China.*

[b]*School of Civil Engineering, Harbin Institute of Technology, Heilongjiang, 150090, P. R. China*

In this study, a series of $LiFePO_4$/CNTs/C composite cathode materials for Li-ion batteries were synthesized by a simple homogeneous precipitation and subsequent annealing process. The investigation of the influence of CNTs on the structural and electrochemical characteristics of $LiFePO_4$/CNTs/C composites shows that the resulting composite material exhibits smaller particle size, lower electron-transfer resistance, and faster lithium ion migration, which are attributed to improve lithium ion transfer by CNT incorporating. At 1C, the $LiFePO_4$/CNTs/C composite delivers a stable specific capacity of ~126 mAh g^{-1} after 500 cycles. At high rates (e.g. 10C), the CNT-incorporated composite is still able to deliver stable capacities of up to ~119 mAh g^{-1}, which is ~42% greater than its pristine counterpart.

Keywords: $LiFePO_4$, CNTs, Composite, Homogeneous precipitation, Li-ion batteries

[1] Corresponding author. Phone: +86-0791-83969514; Email: zyyang@ncu.edu.cn, cjx@ncu.edu.cn

1. Introduction

As an energy storage device, Lithium ion batteries (LIBs) have been widely used in wireless telephones, digital cameras, laptop computers, and other electronic devices since they were first introduced in the 1990s. Recently, the application of LIB technology in electrical energy storage systems for smart grids that are powered by conventional energy sources such as coal, as well as intermittent renewable energy sources such as solar and wind, has attracted considerable attention [1-3].

In the present LIB market, any Li-ion cathode needs to satisfy the demands of high energy density, fast charging capability, long shelf-life and safety. To address these requirements, great efforts have been made to develop phosphate-based cathodes because the strongly covalent $(PO_4)^{3-}$ units provide greater structural stability than commercial $LiCoO_2$ hosts even under deep charging conditions and elevated temperatures [4-7].

Among the known phosphates, olivine $LiFePO_4$ cathode materials are being commercialized due to their low toxicity, low cost, long cycle life and safety. Although the theoretical specific capacity of $LiFePO_4$ is ~170 mAh g^{-1}, its poor rate capability prevents its use in high power applications. Improvements in rate capability have been achieved by enhancing the low electronic conductivity and reported in many research literature, including carbon coating, doping with a conducting metal ion and particle-size control [8-19]. Many kinds of carbon materials (e.g. acetylene black, CNTs, graphene) are used to increase the electronic conductivity of $LiFePO_4$. Larger amounts of carbon materials will increase rate capability and reduce volumetric

energy density of the cathode [18, 20-26]. However, the amount and structure of carbon content will strongly influence the electronic conductivity of $LiFePO_4$/C composite materials. Therefore, to avoid decreasing the volumetric energy density, the amount of carbon should be kept low and more efficient in the industrial applications.

We report here a simple homogeneous precipitation method[27-29] for obtaining $LiFePO_4$/C/CNTs composite with small amount of CNTs and carbon source by (i) homogeneous precipitation of $Fe(NO_3)_3$ in a suspension of CNTs using urea and (ii) subsequent annealing the mixture of the precursors, lithium carbonate (Li_2CO_3), and citric acid at 700 °C for 10 h under a nitrogen atmosphere. As an cathode material for Li-ion batteries, the LiFePO4/C/CNTs composite exhibited a continuous and dispersive nano-carbon network which show the high electronic conductivity and rate capability. Our method of synthesis presents a promising route for large scale production of $LiFePO_4$/C/CNTs composites as electrode materials for Li-ion batteries.

2. Experimental

The $LiFePO_4$/C/CNTs cathode materials were synthesized by homogeneous precipitation of $Fe(NO_3)_3$ in a suspension of CNTs using urea and a subsequent annealing process. Small amount of citric acid was used as both chelating agent and carbon source which used as reductant for iron ions and provides the networked structure of carbon for electronic conduction. All chemicals used in this paper were of analytical grade without any pretreatment.

First, $Fe(NO_3)_3 \cdot 9H_2O$, soluble CNTs, NH_2CONH_2 and $NH_4H_2PO_4$ were mixed uniformly and dissolved in deionized water with continuous magnetic stirring for ~6 hours at ~85 °C under pH = ~3, then the precipitates were obtained (Equation 1). Subsequently, the precipitates was washed with water and dried in an oven at ~120 °C for ~3h. Afterward, the as-prepared precursor together with the lithium carbonate (Li_2CO_3), citric acid ($C_6H_8O_7 \cdot H_2O$) in the molar ratio of 1:0.5:0.1 was mixed in a moderate amount ethanol and ground by ball-milling for 6h, then pre-sintered at □400 °C for □5 h in a flowing N_2 atmosphere. This allowed the formation and release of H_2O and NH_3 as well as CO_2 associated with the decomposition of organic components. Finally, the obtained precursor was carefully grounded after cooling to room temperature, and was calcined at ~700 ^{0}C for ~10 hours to to yield the $LiFePO_4$/CNTs/C composite (Equation 2).

$$Fe(NO_3)_3 + NH_4H_2PO_4 + CNTs \xrightarrow{NH_2CONH_2,(PH\sim3),(85^\circ C)} FePO_4/CNTs\downarrow + NH_4NO_3 \quad (1)$$

$$FePO_4/CNTs + Li_2CO_3 + C_6H_8O_7 \cdot H_2O \longrightarrow LiFePO_4/C/CNTs + CO_2\uparrow + H_2O \quad (2)$$

The crystalline structural characterization of the samples was carried out by X-ray diffraction (XRD) using a diffractometer (Bruker D8 Focus X-ray diffractometer), and the diffraction patterns were recorded at room temperature in the 2θ range between ~10° and ~80°. The morphology and particle sizes of the powders were characterized under a scanning electron microscope (SEM, FEI Quanta200F) and transmission electron microscope (TEM, FEI Tecnai G2 F20, 200 kV).

Electrochemical properties were evaluated with model CR2025 coin-type cell. Cycling and galvanostatic charge–discharge performance of the two-electrode

electrochemical cells were tested on a multi-channel battery test system (Xinwei, Shenzhen, China), while cyclic voltammetry (CV) and electrochemical impedance spectroscopy (EIS) measurements were performed on an electrochemical workstation (PARSTAT 2273, Prinston, USA). For the two-electrode coin battery cell, a lithium metal foil of about 0.3 mm in thickness was used as the anode, and the cathode electrode was prepared as follows: The as-prepared powders, acetylene black and polyvinylidiene fluoride (PVDF) binder in a weight ratio of 80:10:10 were mixed in N-methyl-2-pyrrolidone (NMP) to create a slurry. The resulting slurry was coated on an Al current collector with a thickness of □75 μm. The cathodes were dried in a vacuum furnace at ~65 °C for □20 h, following which they were roll-pressed at a pressure of □15 MPa. Circular electrodes (12 mm in diameter) were then punched out. We measured the average weight of several pure aluminum sheets (12 mm in diameter), and the weight of the dry Al current collector (sheets) of the same size coated with the cathode materials. Then we computed the mass of the cathode materials by subtraction. The typical weight of the cathode ranged between □7 and 8 mg. Finally, the cathode was dried again in a vacuum oven at □100 °C for □48 h prior to assembly. The cells were assembled in a high purity argon atmosphere inside a glove box (Mbraunlab Master130, Germany). Celgard® 2325 was used as the separator and the electrolyte was a solution of 1 M $LiPF_6$ dissolved in a mixture of ethylene carbonate (EC):dimethyl carbonate (DMC) (1:1 vol.%).

3. Result and Discussion

The XRD experiments were conducted to examine the structural changes of $LiFePO_4$/C/CNTs composites by incorporation of various amounts of CNT (x = 0, 1%, 3%, 5%). As shown in Fig. 1, the $LiFePO_4$/C/CNTs composites retained the single phase of $LiFePO_4$. All fundamental peaks could be indexed to the typical olivine structure of $LiFePO_4$ (PDF No.83-2092) and no impurity was revealed [30], which indicates that the incorporation of CNTs did not change the basic crystal structure of $LiFePO_4$. Therefore we expect that CNTs would provide the network structure together with the coated carbon for electronic conduction. Furthermore, the crystallinity of $LiFePO_4$ is maintained even after CNTs involved. This factor is critical as high crystallinity has the potential to significantly improve the cycling stability of the cathode [31, 32].

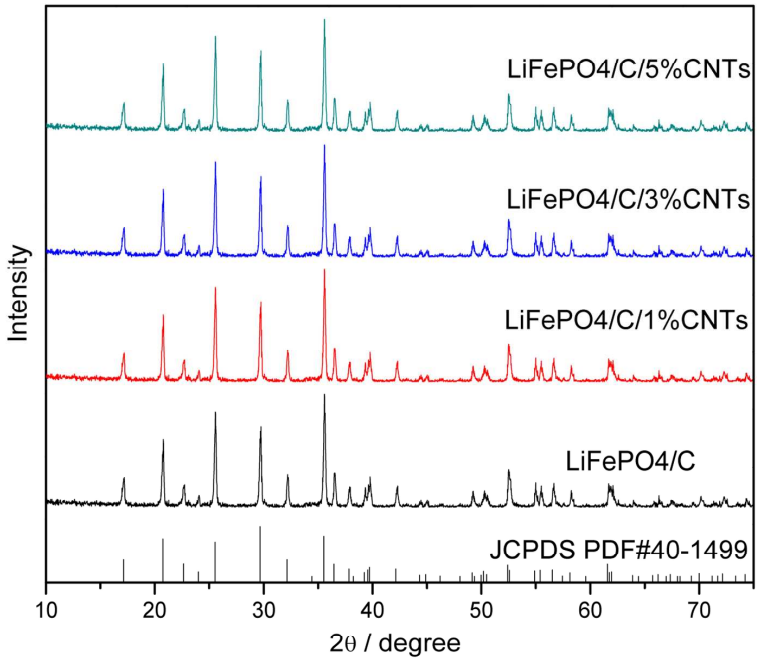

Figure 1. X-ray diffraction patterns of $LiFePO_4$/CNTs/C composites: the amount of CNTs= 0 (a); 1wt% (b); 3 wt% (c); 5 wt% (d).

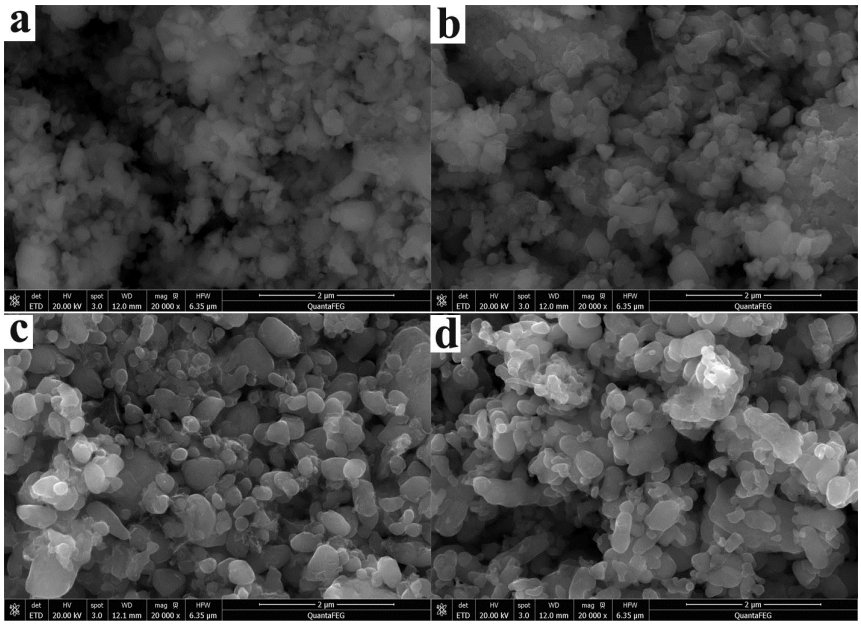

Figure 2. SEM images of $LiFePO_4$/CNTs/C composites: the amount of CNTs= 0 (a); 1wt% (b); 3 wt% (c); 5 wt% (d).

The SEM images of CNTs and pristine $LiFePO_4$/C composites are shown in Fig. 2(a-d), respectively. From SEM observations, the $LiFePO_4$/C sample shows a flake-like morphology, the particles are about 1 μm in diameter and slightly agglomerated with each other as shown in Fig. 2(a) while the size of $LiFePO_4$ /C/CNTs composites (the amount of CNTs = 1 wt%, 3 wt%, 5 wt%) particles is smaller and more uniform compared to the baseline with diameters of less than 500 nm as indicated in Fig. 2(b-d). It indicates that the addition of CNTs influences the geometry and shape of the particles. This result is similar to what has been reported previously [24]. Among the CNTs incorporated samples, the $LiFePO_4$/C composite (3

wt% CNTs) has the smallest particle size (i.e. highest specific surface area) and a uniform morphology; we expect that such a microstructure will facilitate the penetration of the electrolyte ensuring better wettability and thereby shortening the diffusion distance of lithium ions from the cathode bulk phase to the electrolyte[33-35].

The image of TEM and HRTEM of the $LiFePO_4$/C composite (3 wt% CNTs) is shown in Fig. 3(a-d). From the TEM observation, the morphology and particle size of all the samples were found to be consistent with the SEM imaging shown in the previous figure. As compared to the smooth surface of pure $LiFePO_4$, it can be seen that the thickness of the amorphous carbon layer is about ~5 nm on the surface of the $LiFePO_4$ grains (Fig. 3c). The lattice fringes with widths of 0.40 nm and 0.35 nm correspond to the (-210) and (111) plane of $LiFePO_4$, and the (-210) and (111) axes are also indicated in Figure 3c (inset).The same pattern can be observed for all the particles. Then, CNTs would form the network structure together with the coated carbon in the composites, as shown in Fig.3d. CNTs have outstanding electrical conductivity due to their special graphite wall structure. Such a conductive carbon network could provide good grain-to-grain electronic contact, thereby reducing the grain-to-grain electrical contact resistance leading to an improvement in electrochemical properties.

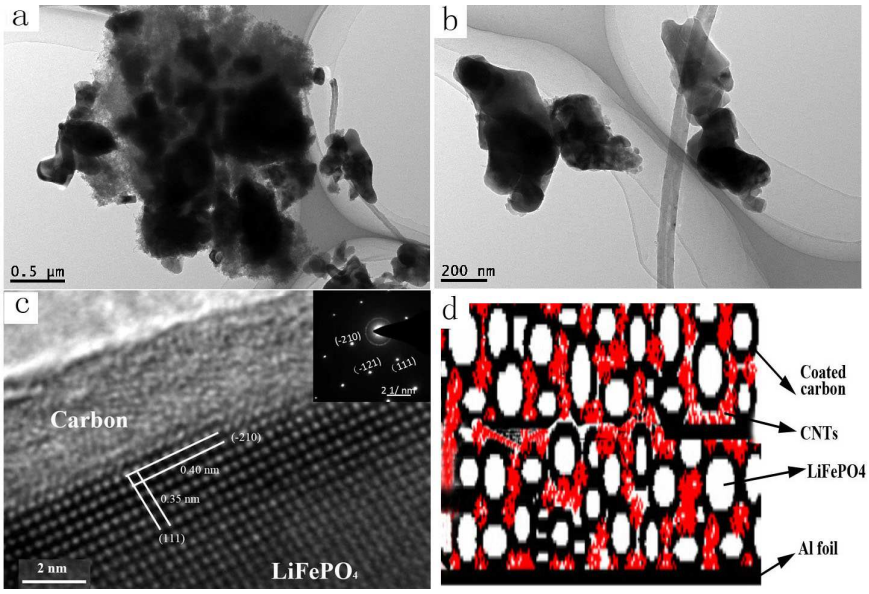

Fig. 3 The image of TEM and HRTEM of $LiFePO_4$/C/3 wt% CNTs composites (a-c); The SAED pattern of LiFeO4 particles (c, inset); Figure Schematic diagram of the structure for $LiFePO_4$/C/CNTs composite athode (d).

The initial charge-discharge curves of $LiFePO_4$/C/CNTs samples (the amount of CNTs=0, ~1 wt%, ~3 wt%, ~5 wt%) at a charge/discharge rate (C-rate) of ~0.1C in the voltage range of ~2.0-4.2 V are presented in Figure 4a. As can be seen in Fig. 4a, almost all the samples obtained exhibit stable voltage plateaus at around ~3.45 V in the charge process, and at around ~3.35V in the discharge process, which correspond to a phase transition processes in $LiFePO_4$ [36]. It can also be seen that the initial discharge capacities of $LiFePO_4$/C/CNTs composites depend on the CNTs amounts. It is found that the charge specific capacities of $LiFePO_4$/C/CNTs (the amount of CNTs =0, 1 wt%, 3 wt%, 5 wt%) are about ~154.3, ~155.7, ~160.8 and ~156.1, mAh g^{-1}, respectively, and the corresponding coulombic efficiencia are ~93%, ~97%, ~97%, and ~94%, respectively. Furthermore, it is found that $LiFePO_4$/CNTs/C composites

exhibits a smaller potential difference between charge and discharge curve. The high coulombic efficiencies are indicative of reversible phase transformations in $LiFePO_4$ associated with lithiation and delithiation steps, thereby ensuring repeatability and reversibility upon successive cycling[31]. However, it is clearly observed that the discharge specific capacity is enhanced considerably when the CNTs amount is ~3wt%. The high discharge capacity of $LiFePO_4$/C/CNTs can be attributed to the decrease of grain size and improved homogeneity as shown in Figs. 2 and 3.

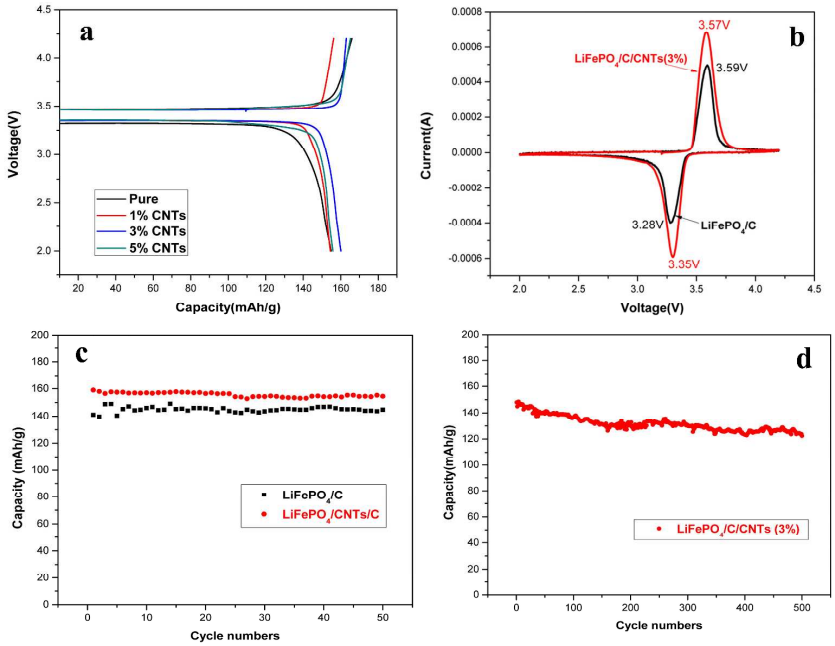

Fig. 4 (a), Charge-discharge tests for $LiFePO_4$ composite samples at 0.1C; (b) Cyclic voltammetry of $LiFePO_4$/C and $LiFePO_4$/C/CNTs; The cycle performance of $LiFePO_4$ composites at 0.1C (c) and 1C (d).

The electrode reaction reversibility of $LiFePO_4$ can also be investigated by the cyclic voltammetry curve. Figure 4b shows the cyclic voltammetry of $LiFePO_4$/C composite and $LiFePO_4$/CNTs/C composite (~3% CNTs) in the second cycle at ~0.1mV/s between 2.0 and 4.2V. A pair of redox peaks and the sharp peaks appears in the curves

for the two samples.The anodic and cathodic peaks are equivalent to the two-phase charge and discharge reaction of the $FePO_4/LiFePO_4$ redox couple. For $LiFePO_4$/C composite, the oxidation and reduction peaks appear at ~3.28V and ~3.59V and the potential interval between the two peaks is ~0.31V. For $LiFePO_4$/CNTs/C composite, the oxidation and reduction peaks appear at ~3.35V and ~3.57V, the potential interval between the two peaks is ~0.22V. The less potential interval indicates that $LiFePO_4$/3%CNTs/C shows a better electrode reaction reversibility. The peak profiles of $LiFePO_4$/CNTs/C composite are more symmetric and it demonstrates a smaller conductivity restriction than that of $LiFePO_4$/C[37-38].

The electrochemical cycling performance of pristine and $LiFePO_4$/~3wt%CNTs/C samples at room temperature and at ~0.1C rate is shown in Fig. 4c. As observed from Fig. 4c, the specific capacities of $LiFePO_4$/C and $LiFePO_4$/C/~3wt%CNTs composites display excellent capacity retention (~100%) with cycle index. When the C-rate increases to ~1C, as shown in Fig 4d, the discharge specific capacity of $LiFePO_4$/ C/~3%CNTs composites still shows the excellent capacity retention, and the discharge specific capacities can still keep about ~126 mAh g^{-1} after 500 cycles. These results indicate that the cycling stability of $LiFePO_4$ can be significantly enhanced by incorporating with optimal amount of CNTs (~3wt%). This improved cycling stability can be attributed to the olive structure of $LiFePO_4$ stabilized by CNTs.

The rate performance of the $LiFePO_4$/C composites and $LiFePO_4$/~3wt%CNTs/C composites is compared in Fig. 5a. For the $LiFePO_4$/C sample, a specific capacity of ~138.2 mAh g^{-1} is obtained at ~1C rate. The specific capacity drops to ~94% of this

value when the operating C-rate is increased to ~2C. The $LiFePO_4$/~3wt%CNTs/C composite delivers ~149.4 mAh g^{-1} at 1C rate and retains a capacity of ~143.0 mAh g^{-1}(~96%) when the C-rate is increased from ~1C to ~2C. However when the rate is increased from ~5C to ~10C, there is a significant difference in the specific capacity between the $LiFePO_4$/C and $LiFePO_4$/~3wt%CNTs/C samples. The specific discharge capacity is ~119.8 mAh g^{-1} (~82%) for the $LiFePO_4$/~3wt%CNTs/C composite, while the pristine $LiFePO_4$/C only shows a specific capacity of ~84.0 mAh g^{-1} (~61%) when the C-rate is ~10C. Faster lithium ion migration and more uniform particle distribution via the homogeneous precipitation method are responsible for the obtained high-rate performance after the ~3wt% CNTs incorporated.

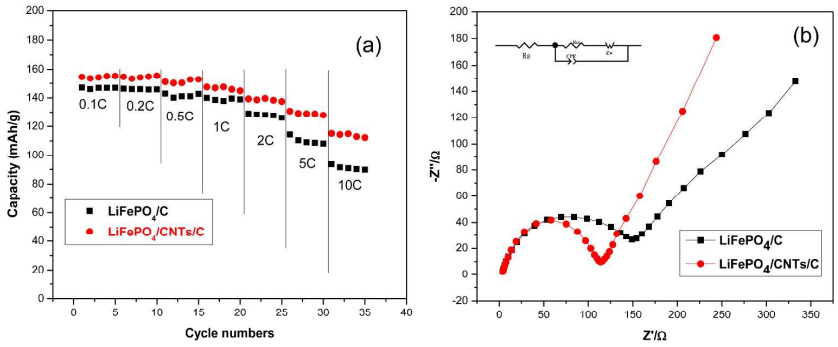

Figure 5. (a) Rate performance of $LiFePO_4$/C and $LiFePO_4$/~3wt%CNTs/C composites, (b) Electrochemical impedance curves of $LiFePO_4$/C and $LiFePO_4$/~3wt%CNTs/C composites.

In order to better understand the kinetics of the $LiFePO_4$/C and $LiFePO_4$/ ~3wt%CNTs/C electrodes, the electrochemical impedance spectra was also measured under fully discharge state after several galvanostatic charge and discharge process

and shown in Fig. 5b. The inset equivalent circuit is used to simulate the impedance spectra. The curve in high frequency corresponds to the interfacial resistance at the surface of the cathode and the intercept is related to the electrolyte resistance (Rs). The semicircle in the medium frequency is related to the charge transfer resistance (Rct), which shows Li^+ interfacial transfer between the interface of $LiFePO_4$ particles and the surface film. The semicircle in low frequency represents the diffusion of Li^+ in the bulk of the electrode and this process is associated with the Warburg impedance (Zw). As shown in Fig. 5, the charge-transfer resistance of the $LiFePO_4$/~3wt%CNTs/C composite (~110 Ω) is significantly lower than that of the $LiFePO_4$/C (~146 Ω), which we expect is associated with the increase in electron conductivity associated with the CNTs introduced.

Another interesting phenomenon obtained from the impedance spectra is the low impedance related to diffusion of lithium ions (low frequency spike) in the $LiFePO_4$/~3wt%CNTs/C composites. The low impedance can be attributed to higher surface area, uniform particle size distribution and better electrolyte wettability associated with homogeneous precipitation of the composite material. The aforementioned factors translate to greater accessibility to active sites for the lithium ions, shorter diffusion distances and quicker lithium ion diffusion, thereby explaining the significantly better rate capability of the $LiFePO_4$/~3wt%CNTs/C composite electrode.

Conclusions

In this work, the $LiFePO_4$/C and $LiFePO_4$/CNTs/C composites have been synthesized by a facile homogeneous precipitation and annealing process. The influence of CNTs on the structural and electrochemical characteristics of $LiFePO_4$/C is analyzed. We show that small amount CNTs can provide the networked structure of carbon for electronic conduction and the resulting composite exhibits small particle size, lower electron-transfer resistance, and faster lithium ion migration kinetics, which are attributed to CNT incorporating. At ~1C, the $LiFePO_4$/~3wt%CNTs/C composite delivers a stable specific capacity of ~126 mAh g^{-1} after 500 cycles. At high rates (e.g. ~10C), the $LiFePO_4$/~3wt%CNTs/C composite is still able to deliver stable capacities of up to ~119 mAh g^{-1}, which is ~42% greater than its pristine counterpart.

Acknowledgements

Z. Yang acknowledges funding support by the National Natural Science Foundation of China (Grant No.20963007, 21263016, 21363015) and Science Research Program in Jiangxi Province (No. GJJ13117, 2011BBE50022) for the financial support.

References

1 M. Armand and J. M. Tarascon, Nature, 2008, 451, 652.

2 L. Shen, H. Li and E. Uchaker, Nano Lett., 2012, 12, 5673.

3 R. Mukherjee, A. V. Thomas and N. Koratkar, ACS Nano, 2012, 6, 7867.

4 R. Mukherjee, A. V. Thomas and E. Singh, Nat. Commun., 2014, 5, 3710.

5 J. W. Kang, V. Mathew and J. Gim, Sci. Rep., 2014, 4, 4047.

6 W. Xu, L. Liu, H. Guo and R. Guo, Electrochim. Acta, 2013, 113, 497.

7 Z. Yang, J. Hu, Z. Chen, RSC Advances, 2015, 5, 17927.

8 A.K. Padhi, K.S. Nanjundaswamy, J.B. Goodenough, J. Electrochem. Soc. 1997, 144, 1188.

9 V. Drozd , G.Q. Liua , R.S. Liua , H.T. Kuo , H. Shenb , D.S. Shy , X.K. Xing, J. Alloys Compd, 2009, 487, 58.

10 P. S. Herle, B. Ellis, N. Coombs, L. F. Nazar, Nat. Mater. 2004, 3, 147.

11 D. Wang, H. Li, S. Shi , X. Huang, L. Chen. Electrochim Acta, 2005, 50, 2955.

12 B. Jin, H.B. Gu, W.X. Zhang , P.H. Park, G.P. Sun. J Solid State Electrochem, 2008, 12, 1549.

13 D. Jugovic, D. Uskokovic, J Power Sources, 2009, 190, 538.

14 K. Dokko, S. Koizumi, K. Sharaishi, K. Kanamura, J Power Sources, 2007, 165, 656.

15 Y. Liu, C. Cao, J. Li, Electrochim Acta, 2010, 55, 3921.

16 O. Makoto, K. Hiroshi, Langmuir, 2002, 18, 4240.

17 O. Toprakci, A.K.H. Toprakci, L. W. Ji, G.J. X, Z. L, X.W. Zhang. Appl. Mater. Interfaces. 2012, 4, 1273.

18 S.W. Kim, J. Ryu, C.B. Park, K. Kang. Chem. Commun, 2010, 46, 7409.

19 B. Jin, E.M. Jin, K.H. Park, H.B. Gu. Electrochem, Commun. 2008, 10, 1537.

20 M. Chen, C. Du, B. Song, K. Xiong, J. Power Sources 2013, 223, 100.

21 Y. Ma, X. Li, Z. Xie, Z. Xiu, Y. Wu, X. Hao, J. Mater. Sci. Mater. Electron., 2014, 25, 2716.

22 S. H. Ha, Y. J. Lee, Chem. Eur. J., 2015, 21, 2132.

23 Z. Ma, Y. Fan, G. Shao, G. Wang, T. Liu, ACS Appl. Mater. Interfaces, 2015, 7, 2937.

24 J. Xu, G. Chen, X. Li, Mater. Chem. Phys., 2009, 118, 9.

25 X. Sun, J. Li, C. Shi, Z. Wang, E. Liu, C. He, J. Power Sources 2012, 220, 264.

26 B. Jin, E. Jin, K.H. Park, Electrochem. Commu. 2008, 10, 1537.

27 Z. Liu, R. Ma, M. Osada, N. Lyi, J. Am. Chem. Soc., 2006, 128, 4872-4880.

28 L. Hu, R. Ma,T.C. Ozawa, T. Sasaki, Angew. Chem. Int. Ed., 2009,48, 3846-3849.

29 L. Hu, R. Ma,T.C. Ozawa, T. Sasaki, Inorg. Chem., 2010,49, 2960-2968 .

30 F. Deng, X.R. Zeng, J.Z. Zou, Chinese Sci Bull, 2011, 56, 1832.

31 L. Yuan, Z. Wang, W. Zhang, J. Goodenough, *Energy Environ. Sci.*, 2011, 4, 269.

32 N. Zhou, E. Uchaker, H. Wang, M. Zhang, RSC Advances, 2013, 3, 19366.

33 J. J. Wang, J. L. Yang, Y. Zhang, Adv, Funct. Mater., 2013,23,806.

34 W. Wei, J. L. Wang, L.J. Zhou, Electrochem. Commu., 2011, 13, 399.

35 Ozan Toprakci, Hatice A.K. Toprakci, L. JI, Acs. Mater. Interfaces, 2012, 4, 1273.

36 X. Zhang, Z. Bi, W. He, G. Yang, Energy Environ. Sci., 2014, 7, 2285.

37 G. X. Wang, H. Liu, J. Liu, Adv. Mater., 2010, 22, 4946.

38 P. Rosaiah, P. J. Kumar, K. J. Babu, O. M. Hussain, Appl phys A, 2013, 113, 610.

Graphical Abstract

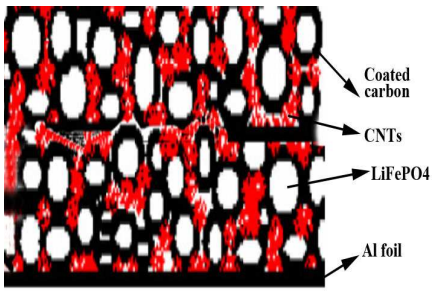

CNTs-doped $LiFePO_4$/CNTs/C composites synthesized by a simple homogeneous precipitation and subsequent annealing process.

CNTs provides the networked structure of carbon for electronic conduction and the resulting composite exhibits small particle size, lower electron-transfer resistance, and faster lithium ion migration kinetics

At 1C, the $LiFePO_4$/CNTs/C composite delivers a stable specific capacity of ~126 mAh g^{-1} after 500 cycles.

At high rates (e.g. 10C), the CNT-doped composite is still able to deliver stable capacities of up to ~119 mAh $g^{-1.}$